

# The Oxygen core inside the Magnesium isotopes

M. Bhuyan

*Institute of Physics, Sachivalaya Marg, Bhubaneswar-751 005, India.\**

(Dated: March 27, 2022)

We have studied the ground state bulk properties of magnesium isotopes using axially symmetric relativistic mean field formalism. The BCS pairing approach is employed to take care of the pairing correlation for the open shell nuclei. The contour plot of the nucleons distribution are analyzed at various parts of the nucleus, where clusters are located. The presence of an  $^{16}\text{O}$  core along bubble like  $\alpha$ -particle(s) and few *nucleons* are found in the Mg isotopes.

PACS numbers: 21.10.Dr, 21.60.-n, 21.60.Jz, 21.60.Gx, 24.10.Jv, 23.70.+j

## I. INTRODUCTION

The internal configuration of a nuclear system plays an important role on the stability, which is connected to the cluster radioactivity. In 1984, the cluster radioactivity was discovered [1] and the consequent excitement led to several experiments at different places all over the world. Finally, *Milano* had developed the experimental technique to investigate such extremely rare mode of decay [2, 3]. Further, the crucial experiments [2, 4, 5] are most notable inputs towards the description of cluster radioactivity. The review of last three decades show a regular interest covering both theory and experiment to explain the aspects of cluster and its exotic radioactivity till date [6].

After the confirmed identification of nuclear sub-structure (clustering), few questions arise in mind: (i) are they initially present inside the parent nucleus (ii) how they look like and (iii) what are the constituent of these clusters. Hence, it is important to see the preformed cluster(s) inside the decaying nucleus. Several techniques are existed in literature to understand the clustering structure of the nuclear system. The prediction of  $3 - \alpha$  structure of  $^{12}\text{C}$  and  $4 - \alpha$  of  $^{16}\text{O}$  are already observed experimentally [7–12]. The presence of these clusters inside a nucleus are due to the random distribution of density. Statistically, the large magnitude in density distribution at cluster region from its surroundings indicates the maximum population of the nucleon(s). This may be a reason for cluster(s) decay. The formation probability and decay half-life of these nuclei have been studied from last three decades by different peoples over the world [13–17]. From these studies, one can find the most possible clusters are  $^4\text{He}$ ,  $^8\text{Be}$ ,  $^{12}\text{C}$ ,  $^{16}\text{O}$ ,  $^{20}\text{Ne}$ ,  $^{24}\text{Mg}$  and  $^{28}\text{Si}$  having  $N = Z$ , which are integral multiple of the  $\alpha$ -cluster ( $n \cdot \alpha$ ). Hence one can say, in case of lighter mass regions, the  $\alpha$ -particle could be the constituent of emitted nuclei. Recently, the theoretical predictions of clusters in lighter mass nuclei [18–22] and some interesting phenomenon such as low-energy spectra of Mg-isotopes [23–27], motivate us to look the the internal configuration of these nuclei using relativistic mean field formalism. In this context, the present work directed to a particular case for Mg isotopes is taken up

to examine the preformed clusters and their constituents. It is worth mentioning that, the RMF theory is very much successful in explaining the sub-atomic nuclei [28–30] and the decays of these nuclei [31, 32]. Because of its applicability, we have used RMF theory with the recently developed  $NL3^*$  [33] and  $NL075$  [34] parameter sets to study the clustering phenomena.

The paper is organized as follows: The relativistic mean field theory is described briefly in Sec. 2 including BCS pairing approach. In Sec. 3, the details of our calculation and results are discussed. Finally, the summary and concluding remarks are given in Section 4.

## II. THE RELATIVISTIC MEAN-FIELD (RMF) METHOD

In last few decades, the RMF theory is applied successfully to study the structural properties of nuclei throughout the periodic table [35–40] starting from proton to neutron drip-lines. The relativistic Lagrangian density for nucleon-meson many-body system is expressed as [38, 40],

$$\begin{aligned} \mathcal{L} = & \bar{\psi}_i \{ i \gamma^\mu \partial_\mu - M \} \psi_i + \frac{1}{2} \partial^\mu \sigma \partial_\mu \sigma - \frac{1}{2} m_\sigma^2 \sigma^2 \\ & - \frac{1}{3} g_2 \sigma^3 - \frac{1}{4} g_3 \sigma^4 - g_s \bar{\psi}_i \psi_i \sigma - \frac{1}{4} \Omega^{\mu\nu} \Omega_{\mu\nu} \\ & + \frac{1}{2} m_\omega^2 V^\mu V_\mu + \frac{1}{4} c_3 (V_\mu V^\mu)^2 - g_\omega \bar{\psi}_i \gamma^\mu \psi_i V_\mu \\ & - \frac{1}{4} \vec{B}^{\mu\nu} \cdot \vec{B}_{\mu\nu} + \frac{1}{2} m_\rho^2 \vec{R}^\mu \cdot \vec{R}_\mu - g_\rho \bar{\psi}_i \gamma^\mu \vec{\tau} \psi_i \cdot \vec{R}^\mu \\ & - \frac{1}{4} F^{\mu\nu} F_{\mu\nu} - e \bar{\psi}_i \gamma^\mu \frac{(1 - \tau_{3i})}{2} \psi_i A_\mu. \end{aligned} \quad (1)$$

Here  $M$ ,  $m_\sigma$ ,  $m_\omega$  and  $m_\rho$  are the masses for nucleon,  $\sigma$ ,  $\omega$  and  $\rho$ - mesons and  $\psi$  is its Dirac spinor. The field for the  $\sigma$ -meson is denoted by  $\sigma$ , for  $\omega$ -meson by  $V_\mu$  and for  $\rho$ -meson by  $R_\mu$ . The coupling constants for  $\sigma$ -,  $\omega$  and  $\rho$ - mesons are  $g_s$ ,  $g_\omega$  and  $g_\rho$ , respectively. The self-coupling constants,  $g_2$  and  $g_3$  are for  $\sigma$ -meson and  $e^2/4\pi=1/137$  is the fine structure constant for photon. From the above Lagrangian we obtained the field equations for the nucleons and mesons. These equations are solved by expanding the upper and lower components of the Dirac spinors and the boson fields in an axially deformed harmonic oscillator basis with an initial deformation  $\beta_0$ . The set of non-linear coupled equations is solved

The center-of-mass motion energy correction is estimated by the usual harmonic oscillator formula  $E_{c.m.} = \frac{3}{4}(41A^{-1/3})$ . The quadrupole deformation parameter  $\beta_2$  is evaluated from the resulting proton and neutron quadrupole moments, as  $Q = Q_n + Q_p = \sqrt{\frac{16\pi}{5}}(\frac{3}{4\pi}AR^2\beta_2)$ . The root mean square (rms) matter radius is defined as  $\langle r_m^2 \rangle = \frac{1}{A} \int \rho(r_\perp, z)r^2 d\tau$ , where  $A$  is the mass number, and  $\rho(r_\perp, z)$  is the deformed density. The total binding energy and other observables are also obtained by using the standard relations, given in [44]. To deal with the open shell nuclei, we have adopted BCS-pairing method in a constant gap approximation [45, 46]. The expression for the pairing energy is given by:

$$E_{pair} = -G \left[ \sum_{i>0} u_i v_i \right]^2, \quad (2)$$

where  $G$  is the pairing force constant and  $v_i^2$  and  $u_i^2 = (1-v_i^2)$  are the occupation probabilities. The variational procedure with respect to the occupation numbers  $v_i^2$ , gives the BCS equation;

$$2\epsilon_i u_i v_i - \Delta(u_i^2 - v_i^2) = 0, \quad (3)$$

and the gap  $\Delta$  is defined by

$$\Delta = G \sum_{i>0} u_i v_i. \quad (4)$$

The occupation number  $n_i$  is defined as

$$n_i = v_i^2 = \frac{1}{2} \left[ 1 - \frac{\epsilon_i - \lambda}{\sqrt{(\epsilon_i - \lambda)^2 + \Delta^2}} \right]. \quad (5)$$

The constant gap pairing for protons and neutrons are taken from Refs. [47]:

$$\Delta_p = RB_s e^{sI-tI^2} / Z^{1/3} \quad \text{and} \quad (6)$$

$$\Delta_n = RB_s e^{-sI-tI^2} / A^{1/3}, \quad (7)$$

with  $R = 5.72$ ,  $s = 0.118$ ,  $t = 8.12$ ,  $B_s = 1$ , and  $I = (N - Z)/(N + Z)$ . The chemical potentials  $\lambda_n$  and  $\lambda_p$  are determined by the particle numbers for protons and neutrons and the pairing energy is given as

$$E_{pair} = -\frac{\Delta^2}{G} = -\Delta \sum_{i>0} u_i v_i. \quad (8)$$

From the Eqn. (8), it is clear that the pairing energy  $E_{pair}$  is not static even in the constant gap approach because it depends on the occupation probabilities  $u_i^2$  and  $v_i^2$ , which is directly connected with the deformation parameter  $\beta_2$  (spherical or deformed) near the Fermi surface. It is well known that  $E_{pair}$  diverges if it is extended to an infinite configuration space for a constant gap  $\Delta$  and strength parameters  $G$ . However, a constant pairing gap is taken for simplicity of the calculations. Within this pairing approach, it is shown that the results for binding energies and quadrupole deformations are almost identical with the predictions of Relativistic-HartreeBogoliubov (RHB) approach [48–53] near the proton-

### III. METHOD OF CALCULATIONS AND DISCUSSIONS

We have carried out the numerical calculations using maximum oscillator quanta  $N_F = N_B = 10$  for Fermion and boson. To test the convergence of the solutions, few calculations are done with  $N_F = N_B = 12$  also. The variation of these two solutions are  $\leq 0.02\%$  on binding energy and  $0.01\%$  on nuclear radii for drip-line nuclei. This implies that the used model space is good enough for the considered nuclei. The number of mesh points for Gauss-Hermite and Gauss-Lagurre integration are 20 and 24, respectively. For a given nucleus, the maximum binding energy corresponds to the ground state and other solutions are obtained at various excited intrinsic states. In our calculations, we obtained different nucleonic potentials, densities, single-particle energy levels, root-mean-square (rms) radii, deformations and binding energies. These observables explain the structure and sub-structure for a nucleus in a given state.

#### A. The Binding Energy and Charge Radius

The nuclear bulk properties are mostly responsible for the internal configuration (arrangement) of the nuclei. In this context, we have calculated the bulk properties like binding energy (BE), nuclear charge radii ( $r_{ch}$ ) and the quadrupole deformation parameter ( $\beta_2$ ) for the ground state of  $^{20-34}\text{Mg}$ . The results obtained from NL3\* and NL075 are compared with the experimental data [54–56] in Table 1. The ground state solution for all the isotopes are followed by a deformed prolate configuration which are comparable with the experimental data [56]. Further, a careful inspection reveal that the prediction of NL3\* for binding energy and radii is slightly better with experimental observation. However, the quadrupole deformation is more closer to the experiment in case of NL075. In general, both the forces predict similar results which are quite close to the experimental values.

#### B. The Clustering and Sub-atomic Nuclei

The internal structure of a nucleus depends on the density distributions of the proton, neutron and matter for a given state. Here, the densities are obtained from RMF (NL3\* and NL075) in the positive quadrant of the plane parallel to the symmetry  $z$ -axis. These are evaluated in the  $\rho z$  plane, where  $\rho = x = y = r_\perp$ . It is to be noted that, both the axes  $z$  and  $\rho$  are conserved in our formalism under the space reflection symmetry. Now we can obtain the complete picture of a nucleus in the  $\rho z$  plane by reflecting the first quadrant to other quadrants. The contour plotting of density along with the color code for the ground state of  $^{24-26}\text{Mg}$  and  $^{28-30}\text{Mg}$  are shown in Figs. 1 and 2, respectively. In the isotopic series, the ground states belong to deformed prolate solution (see Table 1), which is also reflected in the figures. From the color code, one can identify the clustering structures in  $Mg$  nuclei. For example, the color code with deep green corresponds to major sub-nuclei  $\approx 0.18 f_0^{-3}$  and the dark blue color

TABLE I: The RMF (NL3\* and NL075) results for binding energy, the quadrupole deformation parameter  $\beta_2$ , and charge radii for Mg isotopes are compared with the experimental data<sup>47,48,49</sup>. The energy in  $MeV$  and radius in  $fm$ .

Nucleus	RMF (NL3*)			RMF (NL075)			Experiment		
	BE	$\beta_2$	$r_{ch}$	BE	$\beta_2$	$r_{ch}$	BE	$\beta_2$	$r_{ch}$
<sup>20</sup> Mg	135.1	0.02	3.169	133.3	0.04	3.250	134.5 (0.028)		
<sup>22</sup> Mg	166.2	0.39	3.159	164.7	0.46	3.241	168.5 (0.013)	0.58 (0.011)	
<sup>24</sup> Mg	193.5	0.45	3.125	190.1	0.52	3.210	198.2 (0.0002)	0.60 (0.008)	3.057 (0.002)
<sup>26</sup> Mg	212.5	0.33	3.061	209.9	0.51	3.185	215.1 (0.0003)	0.48 (0.010)	3.033 (0.002)
<sup>28</sup> Mg	228.1	0.26	3.061	224.7	0.40	3.159	231.6 (0.002)	0.49 (0.035)	
<sup>30</sup> Mg	240.5	0.56	3.072	236.8	0.23	3.110	241.1 (0.008)	0.43 (0.019)	
<sup>32</sup> Mg	250.5	0.00	3.091	249.2	0.01	3.094	249.7 (0.013)	0.47 (0.043)	
<sup>34</sup> Mg	256.5	0.32	3.149	252.9	0.33	3.159	256.5 (0.238)		

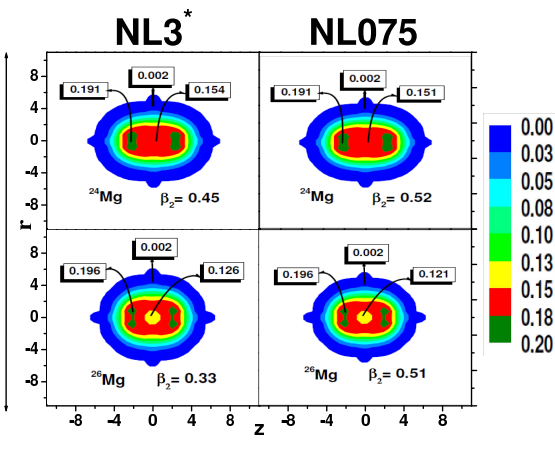


FIG. 1: The internal sub-structure of <sup>24,26</sup>Mg in the ground state configuration.

the minimum value of  $\rho \sim 0.001 fm^{-3}$ . (In black and white figures, the color code is read as deep black with maximum density to outer gray as minimum density distribution). A careful inspection of the figures show the formation of various clusters inside the nuclei. This region has a very high probability of preformation and decaying from its interior. The constituents of this cluster depends on the size and the magnitude of the density of the region. To determine, these sub-nuclear structure (cluster) inside the nucleus, it is important to know the volume of the cluster, i.e., ranges or area covered by the cluster.

The dimension of the cluster is estimated from the contour plot, defines the lower and upper limit of the integral in equation (9) [ $r_{\perp}(r_1, r_2)$  and  $z(z_1, z_2)$ ]. It is worth mentioning that the ranges are fixed by graphical method which is guided

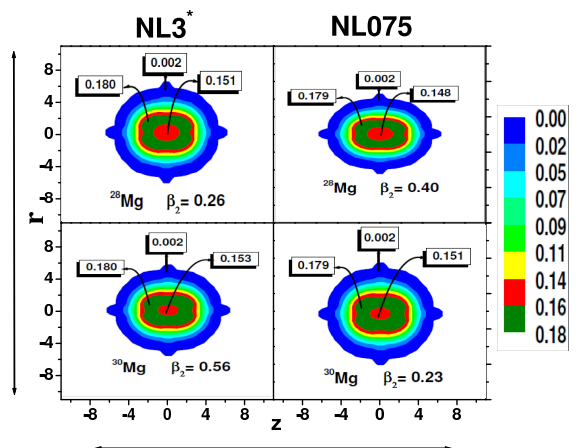


FIG. 2: The internal sub-structure of <sup>28,30</sup>Mg in the ground state configuration.

the ranges for different clusters for some of the Mg isotopes are listed in Table 2. The formula used to identify the ingredient of the cluster is given by [28, 30]:

$$n = \int_{z_1}^{z_2} \int_{r_1}^{r_2} \rho(z, r_{\perp}) d\tau, \quad (9)$$

where,  $n$  is the number of neutrons  $N$  or protons  $Z$  or mass  $A$  and  $z(z_1, z_2)$ ,  $r_{\perp}(r_1, r_2)$  are the ranges. From the estimated proton and neutron numbers, we determine the mass of the cluster inside the nucleus. The obtained clusters for ground state of Mg isotopes are listed in Table 2. From the table, we noticed the presence of <sup>16</sup>O and two <sup>4</sup>He along with few neutrons in <sup>24–30</sup>Mg.

As a further confirmatory test, here we compare the central

TABLE II: The RMF (NL3\*) results for cluster (s) inside the nuclei and the corresponding states along with the range of the cluster and the respective densities are listed.

Nucleus	$\beta_2$	Range ( $r_1, r_2; z_1, z_2$ )	$Z_{clus.}$	$N_{clus.}$	Cluster	Diffused nucleons
RMF (NL3*)						
$^{24}\text{Mg}$	0.45	-1.09,1.09; 2.76,2.82	1.98	2.01	$^4\text{He}$	$8n$ & $8p$
		-1.09,1.09; -1.76,-2.82	1.98	2.01	$^4\text{He}$	
RMF (NL075)						
$^{24}\text{Mg}$	0.52	-1.09,1.09; 2.76,2.82	1.98	2.01	$^4\text{He}$	$8n$ & $8p$
		-1.09,1.09; -1.76,-2.82	1.98	2.01	$^4\text{He}$	
RMF (NL3*)						
$^{26}\text{Mg}$	0.33	-1.1,1.1; 1.68,2.35	1.92	2.03	$^4\text{He}$	$10n$ & $8p$
		-1.1,1.1; -1.68,-2.35	1.93	2.03	$^4\text{He}$	
RMF (NL075)						
$^{26}\text{Mg}$	0.51	-1.1,1.1; 1.68,2.35	1.92	2.03	$^4\text{He}$	$10n$ & $8p$
		-1.1,1.1; -1.68,-2.35	1.93	2.03	$^4\text{He}$	
RMF (NL3*)						
$^{28}\text{Mg}$	0.26	-1.84,1.84; -0.81,0.81	0.06	3.98	$4n$	$4n$ & $4p$
		-1.84,1.84; 2.67,2.67	7.89	8.08	$^{16}\text{O}$	
RMF (NL075)						
$^{28}\text{Mg}$	0.40	-1.84,1.84; -0.81,0.81	0.06	3.98	$4n$	$4n$ & $4p$
		-1.84,1.84; 2.67,2.67	7.89	8.08	$^{16}\text{O}$	
RMF (NL3*)						
$^{30}\text{Mg}$	0.56	-1.99,1.99; 0.81,0.81	0.04	5.98	$6n$	$4n$ & $4p$
		-1.83,1.83; 2.62,2.62	7.89	8.12	$^{16}\text{O}$	
RMF (NL075)						
$^{30}\text{Mg}$	0.23	-1.99,1.99; 0.81,0.81	0.04	5.98	$6n$	$4n$ & $4p$
		-1.83,1.83; 2.62,2.62	7.89	8.12	$^{16}\text{O}$	

of  $Mg$ -isotopes. Normally, the magnitude of the central density of  $^4\text{He}$  and  $^{16}\text{O}$  are  $\sim 0.20$  and  $0.16$ , respectively. Here, the maximum value of the density correspond to these cluster region within the range  $\sim 0.14 - 0.17$ , which matches to the normal density of  $^{16}\text{O}$ . Hence, this confirms, the constituent nucleus inside the cluster (s) region may either  $^{16}\text{O}$  or the condensate  $4 \cdot \alpha$ -particles. It could accept that the present study is a quantitative analysis for the internal structure of  $^{24}\text{Mg}$ . This finding of  $^{16}\text{O}$  and  $^4\text{He}$  bubbles in  $^{24}\text{Mg}$  is irrespective of NL3\* and NL075 forces, which shows the universality of the RMF formalism. As these are preformed clusters inside the nuclei, they may have high decaying probability. The existence of such bubble inside  $Mg$  could be an interesting experimental observation.

#### IV. SUMMARY AND CONCLUSIONS

Concluding, we have presented the gross nuclear properties like binding energy, deformation parameter  $\beta_2$ , charge radii  $r_{ch}$  and the nucleonic density distributions for the isotopic

chain  $^{20-34}\text{Mg}$  using an axially deformed relativistic mean field formalism with  $NL3^*$  and  $NL075$  parameter sets. The results of our calculations show qualitative and quantitative agreement with the experimental observations. We found deformed prolate ground states solution for  $Mg$  isotopes, which are consistent with the experimental data. Analyzing the nuclear density distributions, the internal structure i.e. the clusters of  $Mg$  isotopes are identified. We found sub-structure like  $^{16}\text{O}$  or  $4 \cdot \alpha$  condensate types along with few more neutrons inside  $Mg$  isotopes. It is also noticed that the cluster structure of a nucleus remain unaffected for different force parameters as long as the solution for that nucleus exist. It is interesting to see these evaporation residues like  $^{16}\text{O}$  and  $^4\text{He}$  for  $Mg$ -isotopes in laboratory.

#### Acknowledgments

This work is supported in part by Council of Scientific & Industrial Research (File No.09/153 (0070) /2012-EMR-I).

- [3] D.V. Aleksandro, et al., *JETP Lett.*, **40**, 909, (1984).
- [4] A. A. Ogloblin, R. Bonetti, V. A. Denisov, A. Guglielmetti, M. G. Itkis, C. Mazzocchi, V. L. Mikheev, Yu. Ts. Oganessian, G. A. Pik-Pichak, G. Poli, S. M. Pirozhkov, V. M. Semochkin, V. A. Shigin, I. K. Shvetsov, S. P. Tretyakova, *Phys. Rev. C*, **61**, 034301, (2000).
- [5] R. Blendowske, H. Walliser, *Phys. Rev. Lett.*, **61**, 1930, (1988).
- [6] D. N. Poenaru, W. Greiner, *Institute of Physics Publishing, Bristol*, **1**, (1966).
- [7] A. Tohsaki, H. Horiuchi, P. Chuck, and G. Ropke, *Phys. Rev. Lett.*, **87**, 192501, (2001).
- [8] Y. Funaki, A. Tohsaki, H. Horiuchi, P. Schuck, and G. Ropke, *Phys. Rev. C*, **67**, 051306 (R), (2003).
- [9] Y. Funaki, A. Tohsaki, H. Horiuchi, P. Schuck, and G. Ropke, *Mod. Phys. Lett. A*, **21**, 2331, (2006).
- [10] Robert Roth, *Phys. Rev. C*, **80**, 064324, (2009).
- [11] H. Matsumura and Y. Suzuki, *Nucl. Phys. A*, **739**, 238, (2004).
- [12] T. Wakasa et al., *Phys. Lett. B*, **653**, 173, (2007).
- [13] S. S. Malik and R. K. Gupta, *Phys. Rev. C*, **39**, 1992, (1989).
- [14] D. N. Peonaru, D. Schnabel, W. Greiner, D. Mazilu and R. Gherghescu, *At. Data and Nucl. Data Tab.*, **48**, 231, (1991).
- [15] G. L. Zhang, X. Y. Le, *Nucl. Phys. A*, **848**, 292, (2010).
- [16] G. Royer, Raj K. Gupta, V. Yu Denisov, *Nucl. Phys. A*, **632**, 275, (1998).
- [17] Raj. K. Gupta, M. Balasubramaniam, R. Kumar, D. Singh, S. K. Arun, and W. Greiner, *J. of Phys. G: Nucl. and Part. Phys.*, **32**, 345, (2006).
- [18] M. Chernykh, H. Feldmeier, T. Neff, P. von Neumann-Cosel, and A. Richter, *Phys. Rev. Lett.*, **98**, 032501 (2007).
- [19] E. Epelbaum, H. Krebs, A. Timo Lähde, Dean Lee, and Ulf-G Meiner, *Phys. Rev. Lett.*, **109**, 2012 (2012).
- [20] Lulu Li, Jie Meng, P. Ring, En-Guang Zhao, and Shan-Gui Zhou, *arXiv:1202.0070v1* [nucl-th], (2012).
- [21] Shan-Gui Zhou, Jie Meng, P. Ring, and En-Guang Zhao, *Phys. Rev. C*, **82**, 011301 (R), (2010).
- [22] Yoshiko Kanada-Enyo, Masaaki Kimura, and Akira Ono, *arXiv:1202.1864v1* [nucl-th], (2012).
- [23] J. M. Yao, H. Mei, H. Chen, J. Meng, P. Ring, and D. Vretenar, *Phys. Rev. C*, **83**, 014308, (2011).
- [24] M. Bender, P.-H. Heenen, and P.-G. Reinhard, *Rev. Mod. Phys.*, **75**, 121, (2003).
- [25] T. Nikšić, D. Vretenar, and P. Ring, *Phys. Rev. C*, **73**, 034308, (2006).
- [26] T. Nikšić, D. Vretenar, and P. Ring, *Phys. Rev. C*, **74**, 064309, (2006).
- [27] Eunja Ha and Myung-Ki Cheoun, *Phys. Rev. C*, **88**, 017603, (2013).
- [28] S. K. Patra, R. K. Choudhury, and L. Satpathy, *J. Phys. G: Nucl. Part. Phys.*, **37**, 085103, (2010).
- [29] P. Arumugam, B. K. Sharma, S. K. Patra, and Raj K. Gupta, *Phys. Rev. C*, **71**, 064308, (2005).
- [30] M. Bhuyan, S. K. Patra, P. Arumugam, and Raj K. Gutpa, *Int. J. Mod. Phys. E*, **20**, 1227, (2010).
- [31] BirBikram Singh, S. K. Patra, and Raj K. Gupta, *Phys. Rev. C*, **82**, 014607, (2010).
- [32] BirBikram Singh, B. B. Sahu, and S. K. Patra, *Phys. Rev. C*, **83**, 064601, (2011).
- [33] G. A. Lalazissis, S. Karatzikos, R. Fossion, D. Pena Arteaga, A. V. Afanasjev, P. Ring, *Phys. Lett. B*, **671**, 36, (2009).
- [34] L. Wilets, *Chin. J. Phys.*, **32**, 6 (1994).
- [35] B. D. Serot and J. D. Walecka, *Adv. Nucl. Phys.*, **16**, 1, (1986).
- [36] J. Boguta and A. R. Bodmer, *Nucl. Phys. A*, **292**, 413, (1977).
- [37] C. J. Horowitz and B. D. Serot, *Nucl. Phys. A*, **368**, 503, (1981).
- [38] J. Boguta, H. Stocker, *Phys. Lett. B*, **120**, 289, (1983).
- [39] S. K. Patra and C. R. Praharaaj, *Phys. Rev. C*, **44**, 2552, (1991).
- [40] W. Pannert, P. Ring, and J. Boguta, *Phys. Rev. Lett.*, **59**, 2420, (1986).
- [41] J. Boguta, *Nucl. Phys. A*, **372**, 386, (1981).
- [42] C. E. Price, G. E. Walker, *Phys. Rev. C*, **36**, 354, (1987).
- [43] J. Fink, V. Blum, P.-G. Reinhard, J. A. Maruhn, W. Greiner, *Phys. Lett. B*, **218**, 277, (1989).
- [44] Y. K. Gambhir, P. Ring, and A. Thimet, *Ann. Phys. (N.Y.)*, **198**, 132, (1990).
- [45] M. A. Preston and R. K. Bhaduri, *Structure of Nucleus* (Addison-Wesley, Reading, MA), chap. 8, 309, (1982).
- [46] P. Möller and J. R. Nix, *At. Data and Nucl. Data Tab.*, **39**, 213, (1988).
- [47] D. G. Madland, J. R. Nix, *Nucl. Phys. A*, **476**, 1 (1981).
- [48] S. K. Patra, *Phys. Rev. C*, **48**, 1449, (1993).
- [49] S. K. Patra, M. Del Estal, M. Centelles, and X. Vinas, *Phys. Rev. C*, **63**, 024311, (2001).
- [50] T. R. Werner, J. A. Sheikh, W. Nazarewicz, M. R. Strayer, A. S. Umar, and M. Misu, *Phys. Lett. B*, **335**, 259, (1994).
- [51] T. R. Werner, J. A. Sheikh, M. Mish, W. Nazarewicz, J. Rikovska, K. Heeger, A. S. Umar, and M. R. Strayer, *Nucl. Phys. A*, **597**, 327, (1996).
- [52] G. A. Lalazissis, D. Vretenar, P. Ring, M. Stoitsov, and L. M. Rebledo, *Phys. Rev. C*, **60**, 014310, (1999).
- [53] Z. Ren, Z. Y. Zhu, Y. H. Cai, and G. Xu, *Phys. Lett. B*, **380**, 241, (1996).
- [54] G. Audi, A. H. Wapstra, and C. Thibault, *Nucl. Phys. A*, **729**, 337, (2003).
- [55] I. Angeli, *At. Data and Nucl. Data Tab.*, **87**, 185, (2004).
- [56] S. Raman, C. W. Nestor, JR.,... and P. Tikkanen, *At. Data and Nucl. Data Tab.*, **78**, 1, (2001).